MOLECULAR AND CELLULAR BIOLOGY, Dec. 1993, p. 7652–7665
0270-7306/93/127652-14$02.00/0

Vol. 13, No. 12

Purification, Characterization, and cDNA Cloning of an AU-Rich Element RNA-Binding Protein, AUF1

WEI ZHANG,† BELINDA J. WAGNER, KAREN EHRENMAN, ANDREW W. SCHAEFER,‡ CHRISTINE T. DEMARIA, DINENE CRATER, KRISTIN DEHAVEN, LAURA LONG, AND GARY BREWER*

Department of Microbiology and Immunology, Bowman Gray School of Medicine of Wake Forest University, Winston-Salem, North Carolina 27157-1064

Received 15 July 1993/Returned for modification 25 August 1993/Accepted 8 September 1993

The degradation of some proto-oncogene and lymphokine mRNAs is controlled in part by an AU-rich element (ARE) in the 3′ untranslated region. It was shown previously (G. Brewer, Mol. Cell. Biol. 11:2460–2466, 1991) that two polypeptides (37 and 40 kDa) copurified with fractions of a 130,000 × *g* postribosomal supernatant (S130) from K562 cells that selectively accelerated degradation of c-*myc* mRNA in a cell-free decay system. These polypeptides bound specifically to the c-*myc* and granulocyte-macrophage colony-stimulating factor 3′ UTRs, suggesting they are in part responsible for selective mRNA degradation. In the present work, we have purified the RNA-binding component of this mRNA degradation activity, which we refer to as AUF1. Using antisera specific for these polypeptides, we demonstrate that the 37- and 40-kDa polypeptides are immunologically cross-reactive and that both polypeptides are phosphorylated and can be found in a complex(s) with other polypeptides. Immunologically related polypeptides are found in both the nucleus and the cytoplasm. The antibodies were also used to clone a cDNA for the 37-kDa polypeptide. This cDNA contains an open reading frame predicted to produce a protein with several features, including two RNA recognition motifs and domains that potentially mediate protein-protein interactions. These results provide further support for a role of this protein in mediating ARE-directed mRNA degradation.

The c-*myc* gene is important for the control of cellular growth, differentiation, and transformation (reviewed in references 17 and 41). It belongs to the class of immediate-early genes whose expression is required to drive cells from G_0 to G_1 following stimulation of quiescent cells by growth factors. However, the c-*myc* gene is not unique in terms of having an essential role in cellular growth processes. It has been known for decades that specific and timely changes in the expression of multiple genes are required for proper embryonic development and cell maturation (20). Expression of genes such as c-*myc* seems to be regulated not only at the levels of transcription, attenuation, nuclear processing, and translation but also at the level of mRNA turnover (reviewed in reference 41). Indeed, direct half-life measurements indicated that c-*myc* mRNA has a half-life of 15 to 40 min (19). These and other studies (41) demonstrated that the control of c-*myc* mRNA turnover might be an important means of regulating both the level and the timing of c-*myc* expression.

Many proto-oncogene mRNAs are very unstable. The rapid turnover of c-*myc* mRNA is controlled by sequences in the 3′ untranslated region (3′UTR) or by coding region sequences (reviewed in references 33 and 60). A common feature of many labile mRNAs, such as those for c-*myc*, c-*fos*, and granulocyte-macrophage colony-stimulating factor (GM-CSF), is the presence of an AU-rich element (ARE) in the 3′UTR which is one *cis*-acting element responsible for their rapid degradation (reviewed in reference 3, 48, and 60). It is also noteworthy that the AREs of proto-oncogene mRNAs, such as c-*myc* and c-*fos* mRNAs, tend to have one or more AUUUA motifs within a U-rich context, while cytokine mRNAs tend to have multiple tandem repeats of AUUUA (70). This might be important because under some circumstances, such as T-cell activation, in which lymphokine mRNAs are transiently stabilized, c-*myc* and c-*fos* mRNAs are not stabilized (1, 37, 62).

Functionally, the ARE appears to mediate the sequential deadenylation and cleavage of the body of the mRNA (11, 64, 72). However, single U-to-A mutations in the AUUUA motifs of the c-*fos* ARE indicate that rapid deadenylation does not require intact AUUUA pentanucleotides within this ARE; however, degradation of the body of the mRNA proceeds about fivefold more slowly (64). The motifs responsible for mediating rapid deadenylation are not known. Several groups have identified ARE-binding proteins that might mediate the degradation of these mRNAs (7–10, 24, 40, 46, 69, 74). However, the mechanism(s) by which these proteins influence ARE-directed mRNA turnover is presently unclear.

We and others have used in vitro mRNA decay systems to identify candidate factors that regulate or contribute to the degradation of specific mRNAs. The validity of this approach is highlighted by the fact that in vitro mRNA decay systems reconstitute cellular mRNA decay parameters in four aspects (reviewed in reference 53): (i) the rank order of mRNA decay rates is the same in vitro and in vivo, (ii) mRNA degradation pathways are similar in vitro and in vivo, (iii) in vitro systems reconstitute mRNA turnover regulated by translational inhibitors, and (iv) in vitro systems reconstitute the destabilization of cellular mRNAs induced by infection with herpes simplex virus type 1. Together, these observations suggest that in vitro mRNA decay systems should be useful for identifying factors that contribute to mRNA turnover.

* Corresponding author.
† Present address: Sloan Kettering Institute, New York, NY 10021.
‡ Present address: Department of Neuroscience, Case Western Reserve School of Medicine, Cleveland, OH 44106.

Using an mRNA decay system developed from extracts of K562 cells, we have identified cellular fractions containing activities involved in c-*myc* mRNA degradation (10–12). Rapid degradation of c-*myc* mRNA in vitro required that the mRNA be associated with polysomes (11). Degradation of polysome-associated c-*myc* mRNA could be accelerated by an activity present in a 130,000 × *g* postribosomal supernatant (S130 [12]). The destabilizing activity in the S130 was present in an approximately 25S complex in low-salt buffers and could be dissociated at high salt (0.5 M) to yield an active 7S complex. Two polypeptides of 37 and 40 kDa copurified with the 7S fraction of S130 that accelerated degradation of c-*myc* mRNA in vitro (10). These polypeptides bound the 3′UTRs of c-*myc* and GM-CSF mRNAs and to poly(U). We refer to this activity as AUF1. While the mRNA degradation activity of the 7S fraction was very labile, its RNA-binding activity was stable. In this study, we have purified the polypeptides involved in the RNA-binding activity of AUF1, raised an antibody used to characterize the intracellular properties of these polypeptides, and molecularly cloned a cDNA that encodes the 37 kDa polypeptide.

MATERIALS AND METHODS

Purification of AUF1. S130 was prepared from human erythroleukemia K562 cells (21, 39) by lysis in buffer A {10 mM Tris-HCl [pH 7.6], 1.5 mM magnesium acetate [$Mg(OAc)_2$], 1 mM potassium acetate [KOAc], 2 mM dithiothreitol, 1 μg each of leupeptin and pepstatin A per ml, 0.1 mM phenylmethylsulfonyl fluoride) as described previously (13). Eight grams of S130 protein from 60 liters of K562 cells (approximately 2.5×10^{10} cells in total) was shaken for 5 h at 4°C with 300 ml of heparin-agarose beads (Sigma) which had been equilibrated with buffer A–0.1 M KOAc. Heparin-agarose was washed with 2.5 column volumes of buffer A–0.25 M KOAc. Bound proteins were eluted with 200 ml of buffer A–1M KOAc.

A 1-ml column of poly(U)-agarose (type 6; Pharmacia) was equilibrated with 30 column volumes of buffer A–1 M KOAc. The heparin-agarose eluate was adjusted to 50 μg of poly(C) per ml and loaded onto the poly(U)-agarose column at a flow rate of 30 ml/h at 4°C. The column was washed with 30 column volumes of buffer A–1 M KOAc. Proteins were eluted from the poly(U)-agarose with a step gradient of increasing KOAc concentration (1 to 4.5 M in 0.5 M increments with 3 ml per increment and 1-ml fractions). ARE-binding activity of AUF1 was measured by mobility shift assay as follows. The ^{32}P-labeled ARE-containing probe was 196 nucleotides (nt) of c-*myc* RNA sequence from the 3′UTR (positions 5616 to 5812 [5]) containing the 140-nt c-*myc* ARE (25); it was synthesized by in vitro transcription of *Ssp*I-digested pMycSD3, using SP6 RNA polymerase (10). RNA-binding mixtures contained the RNA substrate and 2 μl of each 1-ml fraction. Free probe and protein-probe complexes were separated on a native 6% polyacrylamide gel and exposed to film. The complexes were scanned by soft-laser densitometry and plotted as percentage of maximum ARE-binding activity. Activity eluted primarily in fractions 15 to 20, corresponding to 3 to 3.5 M KOAc. These fractions were pooled, dialyzed against buffer A–0.1 M KOAc, and concentrated to 200 μl by using a Centricon 30 (Amicon). Typically, 270 μg of AUF1 was obtained from 2.5×10^{10} cells. The amount of AUF1 was determined by sodium dodecyl sulfate (SDS)-polyacrylamide gel electrophoresis (PAGE) and silver staining, using various concentrations of bovine serum albumin (BSA) as standards.

Construction of plasmids and in vitro transcription. Plasmid pGEMmyc(AT1) was derived from plasmid pMycSD3 (10) by introducing a *Sma*I site at the first polyadenylation site by polymerase chain reaction. The *Sac*I-*Sma*I fragment, containing the ARE, was cloned into *Sac*I-*Sma*I-digested plasmid pGEM-7Zf(+) (Promega) such that transcription with SP6 RNA polymerase yields sense RNA. Plasmid pGEMmycARE(mut) was derived from pGEMmyc(AT1) by site-directed mutagenesis. Specifically, the two ATTTA motifs (indicated by the underlines below) were disrupted by single T-to-A mutations (indicated by the boldface letters below), resulting in the sequence 5′-CATCTTTTTTTTTT CTTTAACAGATTTGTATATAAGAA TTGTTTTTAAAAA ATTTTAAGATATACAC-3′. Plasmid pSP64GMΔAU(NcoRI) was derived from pSP64GMΔAU + ATG (30) by digestion with *Nco*I and *Hin*dIII and ligation of the large fragment to produce a plasmid with the human GM-CSF 3′UTR, lacking the 83-nt ARE, in the sense orientation for SP6 transcription. Plasmids pα19Rβ, pα19Rβ+ARE, and pα19Rβ+ARE3 were derived from plasmids pBBB, pBBB+ARE, and pBBB+ARE3 (64), respectively, by cloning the *Eco*RI-*Kpn*I fragment containing the rabbit β-globin 3′ end (and c-*fos* ARE sequences) into the *Eco*RI-*Kpn*I site of plasmid pT7/T3α19 (Bethesda Research Laboratories). In vitro transcription reactions were performed with linearized templates and either SP6, T7, or T3 RNA polymerase (11). [α-^{32}P]UTP was included for synthesis of radiolabeled RNAs.

UV cross-linking analysis. Mixtures contained purified AUF1 protein and 200,000 cpm of probe in a final volume of 10 μl containing 10 mM Tris-HCl (pH 7.5), 2 mM dithiothreitol, 100 mM KOAc, 5 mM $Mg(OAc)_2$, 0.1 mM spermine, and 1 mg of poly(C) per ml. For competition experiments, unlabeled competitor RNAs were added simultaneously with ^{32}P-labeled probe in 5-, 25-, or 250-fold molar excess over labeled probe. Reaction mixes were incubated on ice for 10 min and treated with 254-nm UV light (energy of 0.25 J) for 3 min at a distance of 15 cm in a Stratalinker apparatus (Stratagene). Reaction mixtures were treated with 10 μg of RNase A (Sigma) at 37°C for 30 min to digest free RNA. Proteins were separated by SDS-PAGE (10% gel) under reducing conditions and visualized by autoradiography.

Preparation of anti-AUF1 antibodies. Approximately 50 μg of poly(U)-agarose eluate was injected at each of three 2-week intervals (150 μg in total) into a New Zealand White rabbit. For affinity purification of antibody to p40, a preparative SDS-polyacrylamide gel was run with AUF1 protein [poly(U)-agarose eluate] and transferred to a nitrocellulose sheet. The sheet was stained with India ink to localize p40, which was cut from the membrane with a scalpel. The strip was cut into small pieces and incubated with 1 ml of whole immune serum at room temperature for 2 h. The strip was washed extensively with phosphate-buffered saline (PBS); antibody was eluted with 1 ml of 100 mM glycine (pH 2) and immediately neutralized with 0.1 ml of 1 M Tris. For control experiments, preimmune serum was subjected to the same affinity purification procedure as the immune serum. Both affinity-purified anti-p40 (α-p40) antibody and mock-purified preimmune serum were used at a 1:50 dilution in Western blot (immunoblot) assays; whole sera were used at a 1:10,000 dilution.

Metabolic labeling and immunoprecipitation of AUF1. For metabolic labeling with [^{35}S]methionine, 8×10^6 K562 cells in log phase were harvested, washed, and incubated in 0.8 ml of methionine-free RPMI 1640 with Tran^{35}S-label (ICN)

(final concentration, 150 μCi/ml) for 3 h at 37°C. For metabolic labeling with ^{32}P, cells were washed and labeled in phosphate-free medium containing ^{32}P-phosphoric acid (ICN) (final concentration, 250 μCi/ml) for 3 h at 37°C. The labeled cells were harvested and washed with PBS. The labeled cell pellets were lysed in Nonidet P-40 (NP-40) lysis buffer (150 mM NaCl, 50 mM Tris-HCl [pH 7.5], 1% NP-40) on ice for 30 min. The lysate was sheared through a 22.5-gauge syringe needle 10 times and spun at 10,000 × *g* for 10 min to remove debris.

For each immunoprecipitation, 10^6 cell equivalents of lysate was used. Lysates were precleared as follows. One hundred microliters of lysate was incubated with 5 μl of rabbit preimmune serum on ice for 1 h. Fifty microliters of protein A cell suspension (Sigma) was washed with 0.5 ml of PBS, incubated in 0.5 ml BLOTTO (5% nonfat dry milk) for 30 min, washed twice with 0.5 ml of PBS, and then washed once with 0.5 ml of NET-gel buffer (50 mM Tris-HCl [pH 7.5], 150 mM NaCl, 0.1% NP-40, 1 mM EDTA, 0.25% gelatin, 0.02% sodium azide). The lysate-preimmune serum mixture was added to the blocked protein A cell pellets, mixed and incubated on a turning wheel for 30 min at 4°C, and centrifuged at 12,000 × *g* for 5 min; the supernatant was used for immunoprecipitation as follows. Either mock affinity-purified preimmune serum or affinity-purified α-p40 antibody was added to the lysates. NET-gel buffer was added to a final volume of 0.5 ml; the mixture was incubated on ice for 1 h and then incubated with protein A cells for another hour. The complexes were washed with radioimmunoprecipitation assay (RIPA) buffer (58) three times and with 10 mM Tris-HCl (pH 7.5)–0.1% NP-40 one time. The protein A pellet was suspended in 30 μl of SDS-PAGE loading buffer, boiled for 5 min, and spun, and the supernatant was fractionated by SDS-PAGE (10% gel). Proteins were visualized by autoradiography.

Subcellular fractionation. A 1-liter culture of K562 cells (6×10^8 cells in total) was harvested and washed in RPMI 1640 without serum. All subsequent procedures were performed at 4°C. Cells were lysed in 7.5 ml of buffer A (see above), using a loose-fitting Dounce homogenizer. By phase-contrast microscopy, nuclei were free of cytoplasmic blebs. Nuclei were washed once in buffer A, resuspended in 3 ml of buffer A–0.1 M KOAc, and treated with a sonicator (Ultrasonics, Inc.) at a power setting of 7 for three 15-s bursts on ice. The sonicated extract was centrifuged at 16,000 × *g* for 15 min to pellet debris. The supernatant was saved as the nuclear fraction. The postnuclear supernatant described above was centrifuged at 20,000 × *g* for 15 min. The pellet was washed once in buffer A, resuspended in 3 ml of buffer A, and saved as the mitochondrial fraction. The postmitochondrial supernatant was layered on top of a cushion of 30% sucrose in buffer A and centrifuged at 130,000 × *g* for 2.5 h in an SW50.1 rotor. The supernatant above the pad was saved as the cytosol (S130) fraction. The pellet was washed twice with buffer A and resuspended in 0.3 ml of buffer A by using a glass homogenizer and saved as the polysome fraction. All subcellular fractions were stored as small aliquots at −80°C.

Immunofluorescence microscopy. K562 cells in growth medium were deposited on microscope slides by using a Cytospin (Shandon Southern Products). FS-4 cells were grown on coverslips (10^4 cells per coverslip). Cells were fixed in 3.7% formaldehyde in ethanol for 1 min and washed with PBS. K562 cells were permeabilized with 0.1% saponin in PBS for 30 min, and FS-4 cells were permeabilized with 0.2% Triton X-100 in PBS for 30 min. This was followed by incubation with primary antibody in PBS–3% BSA for 2 h at room temperature. The α-p40 and mock-purified preimmune antibodies were used at 1:10. Anti-β-actin (Boehringer Mannheim) was used at 10 μg/ml. Anti-heterogeneous nuclear ribonucleoprotein C (anti-hnRNP C) was used as an undiluted hybridoma supernatant (provided by Jeff Wilusz) (73). After a wash in PBS, fluorescein isothiocyanate-conjugated goat anti-mouse immunoglobulin G (Sigma) and trimethyl rhodamine isothiocyanate-conjugated goat anti-rabbit immunoglobulin G (Sigma) were added at 1:10 in PBS–3% BSA and incubated at room temperature for 30 min. Slides were washed in PBS and mounted. Fluorescence was observed with a Dialux 30 EB microscope at a magnification of ×60 with oil immersion.

Screening of a HeLa expression library and analysis of fusion proteins. A HeLa λ ZAP II expression library was obtained from Barbara Yoza. Recombinant plaques (600,000 in total) were plated at a density of 30,000 PFU/150-mm plate of *Escherichia coli* BB4. After incubation for 4 h at 42°C, plates were overlaid with nitrocellulose filters soaked in 10 mM isopropyl-β-D-thiogalactoside (IPTG) and incubated for 4 h at 37°C. Replica filters soaked in IPTG were overlaid on the plates and incubated for another 6 h at 37°C. Filters were blocked in BLOTTO (5% nonfat dry milk) and then incubated for 2 h at room temperature with affinity-purified α-p40 antibody (described above) diluted 1:50 in BLOTTO. Filters were washed in PBS and developed with ^{125}I-labeled protein A (ICN). Plaques yielding duplicate positive signals were purified by several rounds of dilution and antibody screening until 100% of the plaques yielded positive signals.

Clones were subcloned into pBluescript by phage rescue. Cell lysates were prepared as described by Zapp and Green (76). Protein was analyzed by SDS-PAGE and Western blotting with α-p40 antibody, by UV cross-linking, and by immunoprecipitation of cross-linked protein.

In vitro translation of AUF1 cDNA. The *Xba*I-*Xho*I fragment of the AUF1 cDNA clone pBS8 was cloned into a derivative of plasmid pGEM-7Zf(+) in which the *Sph*I site in the polylinker was destroyed [to remove an ATG present in the multiple cloning site of plasmid pGEM-7Zf(+)]. AUF1 mRNA was prepared by transcription of the *Xho*I-digested plasmid by using T7 RNA polymerase. RNA was translated in rabbit reticulocyte lysate (Promega) supplemented with 1 mCi of Tran^{35}S-label (ICN) per ml according to the manufacturer's protocol except that compensation buffer [final concentration, 42 mM KOAc–0.75 mM $Mg(OAc)_2$–15 mM triethanolamine] was added. Translation products were fractionated by SDS-PAGE (10% gel) and visualized by autoradiography.

DNA sequence analysis. Overlapping restriction fragments deduced from the restriction map were subcloned into pGEM-7Zf(+) or pGEM 3Z (Promega). To facilitate sequencing of the 3′UTR, the 2.5-kb AUF1 cDNA insert was subcloned into the *Xba*I-*Xho*I sites of pGEM-7Zf(+). Nested deletions of cDNA inserts were prepared by digestion of linearized plasmids with exonuclease III and nuclease S1 (Promega) and intramolecular ligation of the modified plasmids. Sequence across restriction sites used for subcloning and regions inaccessible by universal primer sequencing was obtained by using synthetic oligonucleotides (Operon) and the original $p37^{AUF1}$ cDNA isolate in Bluescript SK+ (Stratagene). Dideoxy sequencing was performed by using Sequenase (U.S. Biochemical). Sequences were merged and analyzed for functional motifs by using the University of Wisconsin Genetics Computer Group software.

Nucleotide sequence accession number. The sequence of $p37^{AUF1}$ has been assigned GenBank accession number U02019.

RESULTS

Isolation and RNA-binding specificity of AUF1. We showed previously that a 7S complex isolated from S130 selectively accelerated degradation of c-*myc* mRNA in an in vitro decay system (10). In the 7S sucrose gradient fractions, ARE-binding activity was associated with two polypeptides of 37 and 40 kDa. We designed a large-scale purification scheme based on the poly(U)-binding activity of these polypeptides. S130 was fractionated by column chromatography using heparin-agarose followed by poly(U)-agarose (see Materials and Methods). For the poly(U)-agarose step, a gradient of increasing KOAc concentration was used to elute bound polypeptides. RNA-binding activity was assayed by gel mobility shift using a ^{32}P-labeled region of the human c-*myc* 3′UTR containing the ARE (10). Maximal ARE-binding activity eluted from the affinity matrix at 3.0 to 3.5 M KOAc in fractions 15 to 20, which were pooled, dialyzed, and concentrated for use in all experiments.

Fractionation of S130 by heparin-agarose and poly(U)-agarose resulted in the isolation of a 40 kDa polypeptide and a 36/37-kDa doublet as well as 29-kDa, 75-kDa, and additional minor polypeptides (Fig. 1A, lane 2). Only the 40- and 36/37-kDa polypeptides reproducibly copurified during poly (U)-agarose chromatography, gel filtration using Sephacryl S300 chromatography, and C8 reverse-phase high-pressure liquid chromatography (data not shown). Several observations indicate that these polypeptides are common to both the 7S sucrose gradient fractions and the poly(U)-agarose eluate. (i) Immunoblotting of the poly(U)-agarose eluate with antibody prepared against the 7S sucrose gradient fractions detected only the 37- and 40-kDa polypeptides (data not shown). (ii) The native molecular size of the ARE-binding activity in the poly(U)-agarose eluate is 150 to 200 kDa by gel filtration, consistent with the 7S sedimentation of the sucrose gradient-purified ARE-binding activity (10). (iii) The 40- and 36/37-kDa polypeptides isolated by poly(U)-agarose demonstrated the same RNA-binding specificity as the sucrose gradient-purified activity (Fig. 1) (10).

To examine RNA-binding specificity, the poly(U)-agarose eluate (Fig. 1A, lane 2) was mixed with ^{32}P-labeled RNA substrates. Partial sequences of selected target RNAs are shown in Fig. 2. Following incubation to permit binding, the mixture was irradiated with 254-nm light and then treated with RNase A. Cross-linked proteins were separated by SDS-PAGE and visualized by autoradiography (Fig. 1A). The 40- and 36/37-kDa species cross-linked efficiently to AUUUAUUUAUUUAUUUA [$(AUUUA)_4$; Fig. 1A, lanes 3 and 4], while the 29- and 75-kDa polypeptides did not efficiently cross-link (compare the silver-stained polypeptide profile in lane 2 with lanes 3 and 4). None of these polypeptides bound RNA with random sequence (lanes 5 and 6) or the rabbit β-globin 3′UTR (lanes 15 and 16), indicating specific binding to $(AUUUA)_4$. The 75-, 40-, and 36/37-kDa species also efficiently cross-linked to both the wild-type c-*myc* ARE and a mutant in which both AUUUA pentanucleotides were disrupted by single U-to-A point mutations (lanes 7 and 8 and lanes 9 and 10, respectively). Likewise, the 75-, 40-, and 36/37-kDa species efficiently cross-linked to the wild-type c-*fos* ARE and a mutant in which all three AUUUA pentanucleotides were disrupted by single U-to-A point mutations (lanes 17 and 18 and lane 19 and 20, respectively). Binding of the 29-kDa species to the c-*myc* and c-*fos* RNAs was negligible. The 75-, 40-, and 36/37-kDa species also efficiently cross-linked to the wild-type GM-CSF ARE (lanes 11 and 12). In contrast, cross-linking of the 40- and 36/37-kDa species to a mutant lacking 83 nt encompassing the GM-CSF ARE was 15% of that observed with wild-type ARE (compare lane 13 with lane 11) (30). However, the 75-kDa species cross-linked to the GM-CSF deletion mutant with the same efficiency as to the wild-type sequence (compare lane 13 with lane 11). This finding suggests that binding of the 75-kDa polypeptide is not specific for the ARE; it was not further investigated in this study. Likewise, because of the inefficient cross-linking of the 29-kDa species to the ARE, this protein was not investigated further. On the basis of the previous cosedimentation data (10) and the chromatographic and UV cross-linking data (shown here), we refer to the 40- and 36/37-kDa species collectively as AUF1.

To confirm the specificity of binding by AUF1, various unlabeled competitor RNAs were added to UV cross-linking assays containing ^{32}P-labeled $(AUUUA)_4$ as the substrate. A 250-fold molar excess of ARE RNAs (wild type and mutant) reduced binding by AUF1 to 1 to 12% of maximum binding (Fig. 1B, lanes 2 to 16 and 20 to 26; Fig. 1C and D), while β-globin reduced binding by only 50% (Fig. 1B, lanes 17 to 19; Fig. 1C and D). Collectively, the UV cross-linking experiments indicate that (i) AUF1 binds to RNA containing AUUUAUUUAUUUAUUUA and to ARE of c-*myc*, c-*fos*, and GM-CSF; and (ii) in the context of the c-*myc* or c-*fos* ARE, intact AUUUA pentanucleotides are not required for binding. In this regard, it is noteworthy that for the c-*fos* ARE, intact AUUUA pentanucleotides are not required for rapid deadenylation (60). To our knowledge, the role of AUUUA pentanucleotides in deadenylation of c-*myc* and GM-CSF mRNAs is not yet known. Nonetheless, the correlations between binding by AUF1 to wild-type AREs and rapid degradation of the mRNAs in vivo strongly suggest that AUF1 participates in ARE-directed mRNA degradation (see Discussion).

Immunological characterization of AUF1. AUF1 was used to immunize a rabbit for production of polyclonal antiserum. A monospecific α-p40 antibody was prepared by affinity purification as described in Materials and Methods. Preimmune serum was mock affinity purified by a procedure identical to that for preparation of α-p40. Sera were tested in a Western blot assay with nitrocellulose strips containing electrophoretically separated total cell protein from K562 cells. Neither preimmune nor mock affinity-purified preimmune serum reacted with any polypeptides (Fig. 3A, lanes 1 and 3). Both whole immune serum and affinity-purified α-p40 antibody detected three polypeptides of 37, 40, and 45 kDa (lanes 2 and 4, respectively). This result suggests that the three polypeptides are immunologically related. The 36-kDa species is not detected in this assay. (We also note that neither the whole sera nor the α-p40 antibody reacted with the 75-kDa polypeptide which cross-linked to some RNA substrates [Fig. 1A and B].) Because the 45-kDa band (p45) was unexpected, Western blots of total cell protein and purified AUF1 were compared by using α-p40. No p45 was detected in purified AUF1 preparations under conditions in which it was readily detected in total protein (Fig. 3B, lanes 1 and 2). To confirm that p45 was immunologically related to p37/p40, α-p40 antibody was preincubated with various amounts of purified AUF1 and then reacted with nitrocellulose strips of total protein. Incubation with purified AUF1 resulted in a loss of reactivity of α-p40 with p45 and p40; p37

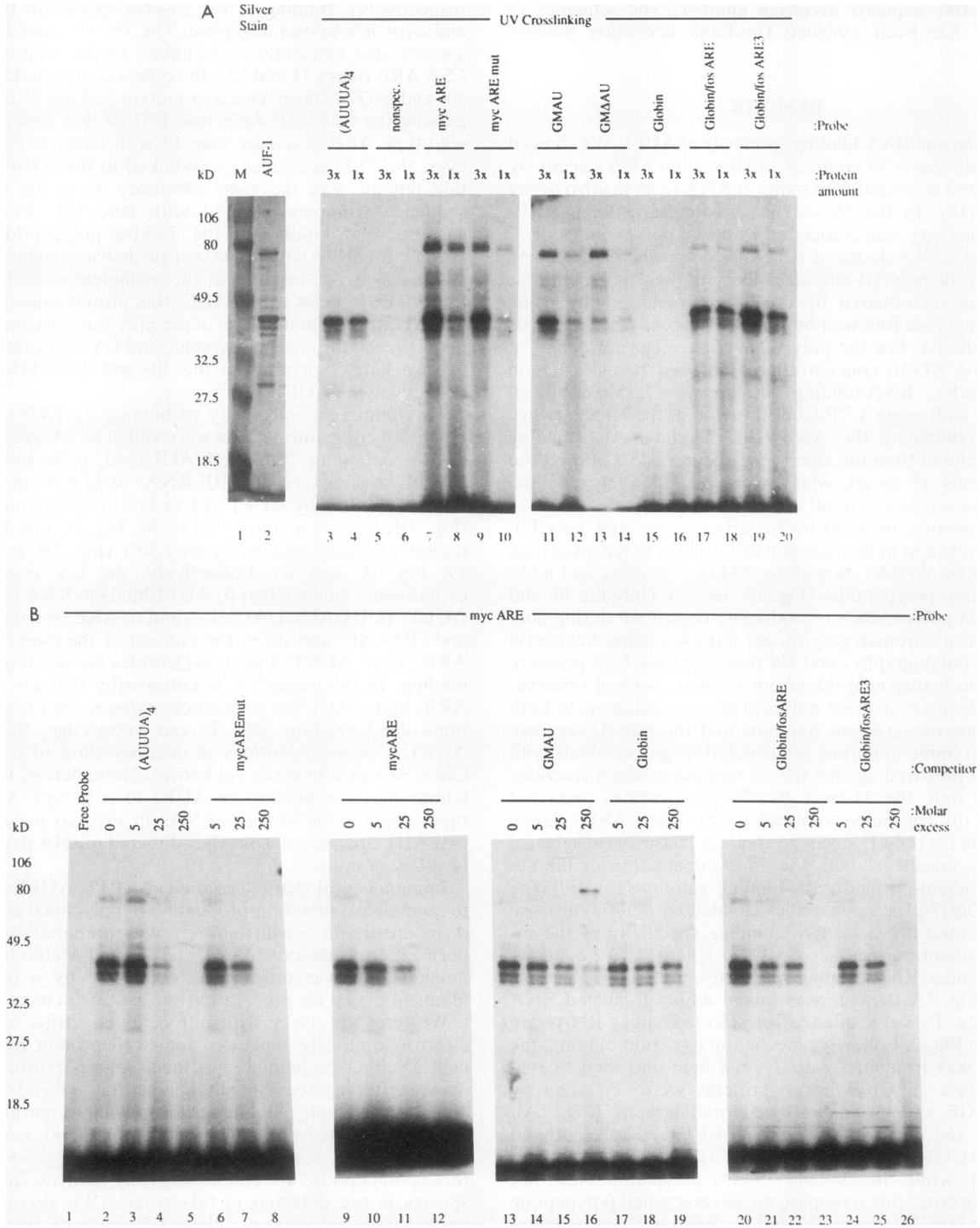

FIG. 1. Analysis of RNA binding by AUF1. (A) UV cross-linking of AUF1 to RNA substrates. AUF1 protein from the poly(U)-agarose column was silver stained (lane 2) or UV cross-linked to equal counts per minute of the ^{32}P-labeled RNA substrates indicated above each pair of lanes (lanes 3 to 20). Mixtures contained either 1× or 3× amounts of protein to ensure probe excess. Following incubation, mixtures were irradiated with 254-nm UV light and treated with RNase A as described in Materials and Methods. Protein cross-linked to ^{32}P-labeled RNA was identified by SDS-PAGE and autoradiography. Plasmid templates were as follows. Plasmid pα19d2 (40) digested with *Eco*RI and transcribed with T7 RNA polymerase produces 76-nt $(AUUUA)_4$ RNA containing the sequence AUUUAUUUAUUUAUUUA. Plasmid pT7/T3α19 digested with *Eco*RI and transcribed with T7 RNA polymerase produces 59-nt nonspecific (nonspec.) RNA. Plasmid pGEMmyc(AT1) digested with *Ssp*I and transcribed with SP6 RNA polymerase produces 227-nt *myc* ARE RNA. Plasmid pGEMmycARE-(mut) digested with *Ssp*I and transcribed with SP6 RNA polymerase produces 227-nt mutant (mut) c-*myc* RNA. Plasmid pSP64GM(NcoRI) digested with *Eco*RI and transcribed with SP6 RNA polymerase produces a 230-nt GMAU RNA (10). Plasmid pSP64GMΔAU(NcoRI) digested with *Eco*RI and transcribed with SP6 RNA polymerase produces 147-nt GMΔAU mutant GM-CSF RNA. Plasmid pα19Rβ digested with *Bgl*II and transcribed with T3 RNA polymerase produces 70-nt globin 3′UTR RNA. Plasmid pα19Rβ+ARE digested with *Bgl*II and

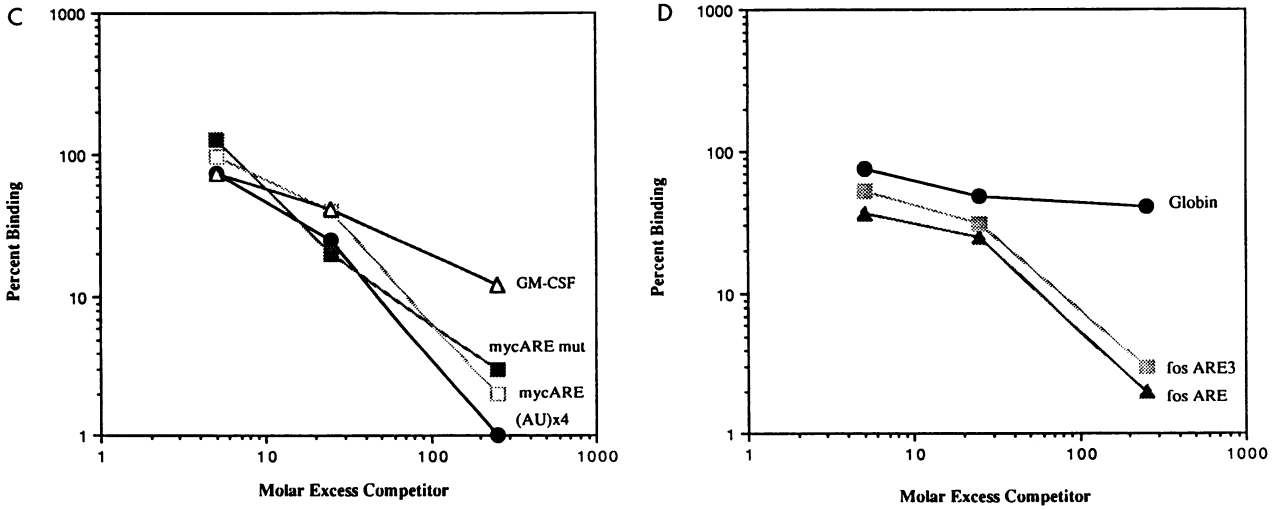

transcribed with T3 RNA polymerase produces 145-nt globin/*fos* ARE RNA. Plasmid pα19Rβ+ARE3 digested with *Bgl*II and transcribed with T3 RNA polymerase produces 145-nt globin/*fos* ARE3 mutant c-*fos* RNA. M, molecular size markers. (B) Competition experiments with ^{32}P-labeled $(AUUUA)_4$. AUF1 and ^{32}P-labeled c-*myc* ARE substrate were mixed simultaneously with 5-, 25-, or 250-fold molar excess of unlabeled RNAs as indicated above the lanes. Following incubation, mixtures were irradiated and treated with RNase A as described above. Proteins were visualized by SDS-PAGE and autoradiography. Molecular sizes are indicated at the left. (C and D) Quantitation of RNA-binding activity. The autoradiographs in panel B were scanned by soft-laser densitometry. The percent binding (compared with no competitor) is plotted versus the molar excess of competitor indicated to the right of each curve.

was too faint to observe (Fig. 3C). Again, this finding suggests that p45 is immunologically related to p37/p40.

We also considered the possibility that p45 could be due to re-formation of intramolecular disulfide bonds in p37 or p40 during the process of gel electrophoresis of total cellular protein, resulting in their aberrant migration. For example, this phenomenon occurs with microsomal signal peptidase as shown by Evans (22). To determine whether this occurs for AUF1, protein samples were treated with iodoacetamide to alkylate sulfhydrals prior to electrophoresis; this prevents re-formation of disulfide bonds (22). The same pattern of bands was observed with or without alkylation (data not shown). This finding suggests that p45 was not due to aberrant migration of p37 or p40. These data, together with the immunological results presented above, suggest that p37, p40, and p45 are immunologically related.

To demonstrate that the α-p40 antibody reacted with an ARE-binding protein, UV cross-linking experiments were combined with immunoprecipitation. AUF1 protein was mixed with ^{32}P-labeled c-*myc* ARE, irradiated with UV light, and treated with RNase A as described for Fig. 1. Reactions were immunoprecipitated with either α-p40 or mock affinity-purified preimmune antiserum. Polypeptides were visualized by SDS-PAGE and autoradiography. Polypeptides of 37 and 40 kDa were observed following immunoprecipitation with α-p40 but not with mock-treated preimmune antiserum (Fig. 3D, lanes 1 and 2). We conclude that the α-p40 antibody recognizes the 37- and 40-kDa RNA-binding species of AUF1.

To determine whether these polypeptides are phosphorylated, K562 cells were metabolically labeled with either [^{35}S]methionine or ^{32}P-labeled phosphoric acid. Lysates were immunoprecipitated with α-p40 antibody and analyzed by SDS-PAGE. The ^{35}S lysate clearly shows the 40-kDa species and, to a lesser extent, the 37- and 45-kDa species; the ^{32}P lysate shows the 40- and 45-kDa species and, to a lesser extent, the 37-kDa species (Fig. 4; compare lane 3 with lane 4). Immunoprecipitation control lanes showed no polypeptides in this size range (lanes 1 and 2). Together, these results indicate that each polypeptide is phosphorylated. However, treatment of cell lysates with potato acid phosphatase did not reduce the three species to a single species. Moreover, phosphatase treatment did not ablate the RNA-binding activity of AUF1 (data not shown). This finding suggests that phosphorylation of AUF1 is not required for RNA-binding activity.

c-myc ARE

CAUCUUUUUUUUUUCUUUAACAGAUUUGUAUUUAAGAAUUGUUUUUAAAAAAUU

UUAAGAUUUA

c-fos ARE

UUUUAUUGUGUUUUUAAUUUAUUUAUUAAGAUGGAUUCUCAGAUAUUUAUAUU

UUUAUUUUAUUUUUUU

GM-CSF ARE

AUGGUGGGAGUGGCCUGGACCUGCCCUGGGCCACACUGACCCUGAUACAGGCAUG

GCAGAAGAAUGGGAAUAUUUUAUACUGACAGAAAUCAGUAAUAUUUAUAU

AUUUAUAUUUUAAAAUAUUUAUUUAUUUAUUUAUUUAAGUUUCAUAUU

CCAUAUUUAUUCAAGAUGUUUUACCGUAAUAAUUAUUAUUAAAAAUAUGCUUCUA

FIG. 2. Partial sequences of RNA-binding substrates containing ARE used in UV cross-linking to AUF1. The AREs from human c-*myc*, c-*fos*, and GM-CSF are shown. For c-*myc* and c-*fos*, the bold and underlined nucleotides were changed to A residues by site-directed mutagenesis for the mutant RNA substrates. These mutant sequences are designated myc AREmut and globin/fos ARE3, respectively, in Fig. 1. (Plasmids for wild-type and mutant c-*fos* were provided by Ann-Bin Shyu.) For GM-CSF, the bold and underlined nucleotides were deleted in the mutant substrate. (Plasmids for wild-type and mutant GM-CSF were provided by Gray Shaw.)

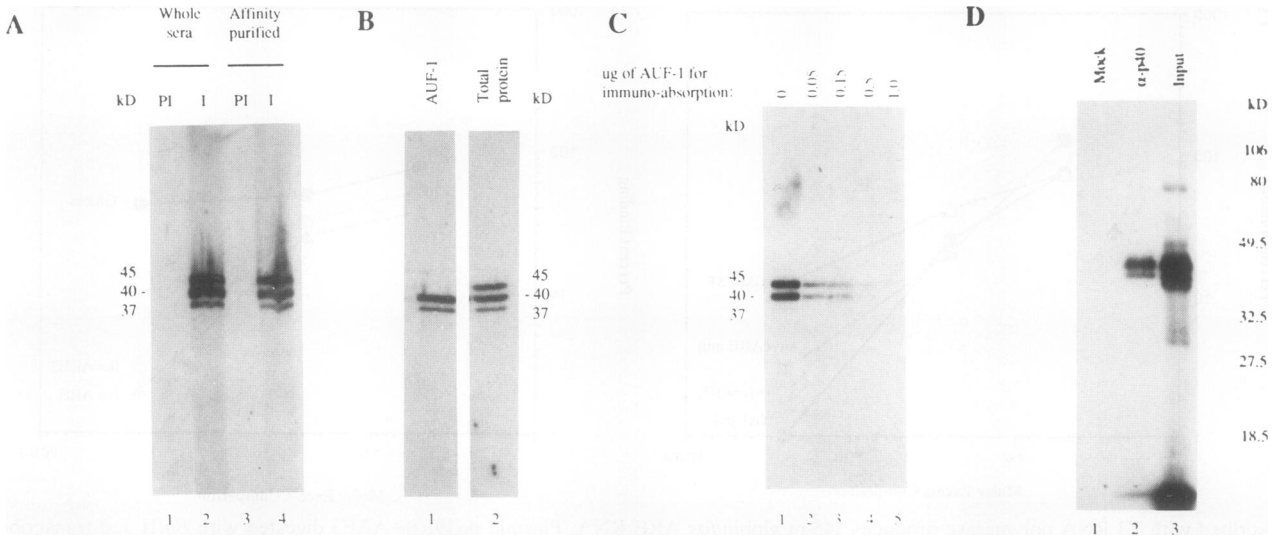

FIG. 3. Characterization of an anti-AUF1 polyclonal antibody. Immune rabbit serum was prepared by using the poly(U)-agarose eluate fractions 15 to 20 (Materials and Methods) as the immunogen. Affinity purification of α-p40 antibody was performed as described in Materials and Methods. Preimmune serum was also subjected to the affinity purification procedure. (A) Test of whole sera and affinity-purified antibodies. Nitrocellulose strips of K562 total cell protein were incubated with either whole sera (preimmune [PI] in lane 1 and immune [I] in lane 2) or affinity-purified antibody (mock in lane 3 and α-p40 in lane 4). The blot was developed with ^{125}I-protein A. (B) Comparison of AUF1 and total K562 cell protein. Separate strips of AUF1 (lane 1) and total cell protein (lane 2) were tested with α-p40 antibody by Western blotting. (C) Immunoabsorption of α-p40 antibody with purified AUF1 protein. Affinity-purified α-p40 antibody was incubated with the indicated amounts of purified AUF1 in a final volume of 60 μl overnight at 4°C. The antibody was then diluted 50-fold to test each nitrocellulose strip of total cell protein by Western blotting. The locations of 45-, 40-, and 37-kDa polypeptides are indicated. (D) UV cross-linking and immunoprecipitation analysis. AUF1 was cross-linked to ^{32}P-labeled c-*myc* ARE and treated with RNase A as described for Fig. 1. Reactions were either not precipitated (lane 3) or immunoprecipitated with mock-purified preimmune serum (lane 1) or α-p40 antibody (lane 2). Polypeptides were visualized by SDS-PAGE and autoradiography.

It is also noteworthy that immunoprecipitation of ^{35}S-labeled proteins with α-p40 antibody resulted in the coprecipitation of 75-, 120-, and 126-kDa polypeptides (p75, p120, and p126, respectively; Fig. 4, lane 3) and 55- and 106-kDa phosphopeptides (pp55 and pp106, respectively; lane 4). Two controls indicate that the coimmunoprecipitation is not simply due to cross-reactivity of the α-p40 antibody with these polypeptides. (i) Following addition of 1% SDS and 1 mM EDTA, lysate was heated at 90°C for 8 min to disrupt protein-protein interactions. After cooling, the treated extract was immunoprecipitated with α-p40. This treatment prevented precipitation of all but the AUF1 polypeptides and p45 (data not shown). (ii) The additional polypeptides are not detected by Western blot analysis with α-p40 antibody, again suggesting that they do not cross-react with the antibody (Fig. 3A and B). Together, these results suggest that AUF1 associates with other cellular proteins; the identification of these additional proteins is under investigation (see Discussion).

Subcellular localization of p37, p40, and p45. Antibodies to p40 reacted with p37, p40, and p45 in total cellular protein, yet p45 was not detected in purified AUF1 (Fig. 3). We therefore examined the subcellular location of each polypeptide by Western blot analysis of 10^6 cell equivalents of nuclear, mitochondrial, polysomal, and cytosolic (S130) fractions of K562 cells with α-p40 antibody. p37 and p40 were present in the nucleus (Fig. 5, lane 5) and cytoplasm, notably in the polysome fraction (lanes 6 to 8). However, p45 was located exclusively in the nuclear fraction (lane 5). This might explain why p45 was not detected in AUF1, since AUF1 was purified by using a cytoplasmic fraction as the starting material. As a control for the subcellular fraction-

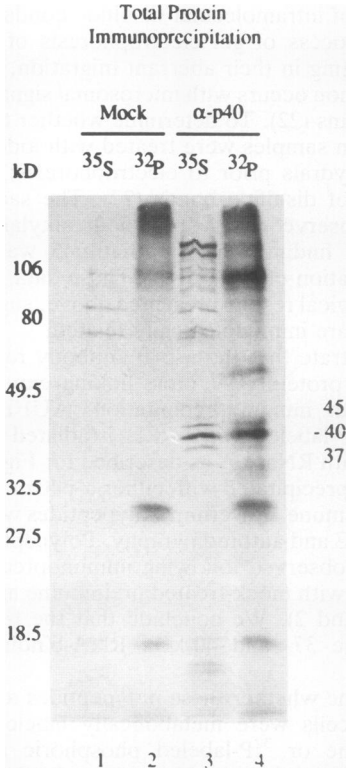

FIG. 4. AUF1 is phosphorylated. Lysates were prepared from K562 cells metabolically labeled with either [^{35}S]methionine (lanes 1 and 3) or ^{32}P (lanes 2 and 4) and immunoprecipitated with either mock, affinity-purified preimmune serum (lanes 1 and 2) or α-p40 antibody (lanes 3 and 4). Immune complexes were subjected to SDS-PAGE, and polypeptides were visualized by autoradiography.

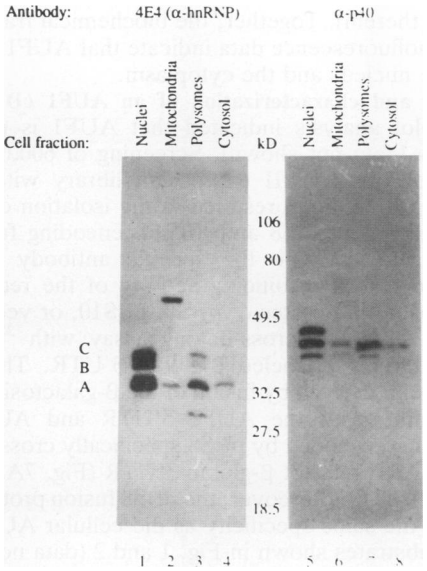

FIG. 5. Subcellular localization of AUF1 polypeptide species. K562 cells were lysed and separated into fractions containing nuclei, mitochondria, polysomes, and cytosol (S130) as described in Materials and Methods. Equal (10^6) cell equivalents of the indicated fractions were separated by SDS-PAGE on the same gel and analyzed by Western blotting with either monoclonal antibody 4E4 (73), which recognizes hnRNP A1/A2, B1/B2, and C1/C2 proteins (lanes 1 to 4), or affinity-purified α-p40 (lanes 5 to 8). The locations of the hnRNP A, B, and C proteins and molecular weight markers are indicated.

ation, fractions were analyzed by Western blot assay using monoclonal antibody 4E4, which reacts with the human hnRNP A1/A2, B1/B2, and C1/C2 polypeptides (73). These polypeptides were predominantly nuclear (lanes 1 to 4) as reported previously (49, 50). The presence of these hnRNP proteins in various cytoplasmic fractions (albeit at lower amounts than in the nuclear fraction) is consistent with their presence in the cytoplasm as a result of shuttling between the nucleus and cytoplasm (50). These results suggest that p37 and p40 did not leak from the nucleus during fractionation procedures. Further confirmation of this is suggested by the restricted localization of p45 to the nucleus.

The distribution of AUF1 was also examined by indirect immunofluorescence. The results of this experiment (Fig. 6) support the intracellular distribution obtained by biochemical fractionation. The localization of a representative nuclear antigen, hnRNP C, is shown in Fig. 6B and E. The grainy, reticular staining was excluded from the nucleoli in both K562 (Fig. 6B) and FS-4 (Fig. 6E) cells and is typical of nuclear matrix-associated and hnRNP antigens (16, 36). Little, if any, hnRNP C staining was observed in the cytoplasm of either cell type. AUF1 in the nuclei of both cell types stained with a pattern similar to that observed for the hnRNP C protein (Fig. 6A and D).

An antibody to β-actin was used to determine the extent of the cytoplasm of K562 cells. In contrast to the abundant, well-spread cytoplasmic area of fibroblasts like FS-4 cells, the cytoplasm of K562 cells was restricted to a thin shell about the nucleus (Fig. 6C). Consequently, although cytoplasmic staining for AUF1 is observed in K562 cells (Fig. 6A), little information about the localization and amount of AUF1 in the cytoplasm can be derived from the immunofluorescence data because of the limited cytoplasmic area. However, in the FS-4 cells, AUF1 staining appears to be widely distributed throughout the cytoplasm. The increased staining observed about the nucleus of these cells might reflect the superposition of staining from the thicker regions of the cell. Nonetheless, it might be significant that a similar cytoplasmic distribution has been reported for polyribosomes in 3T3 cells and a number of mRNA species, such as histone mRNA, in a variety of cells (references 35 and 65 and

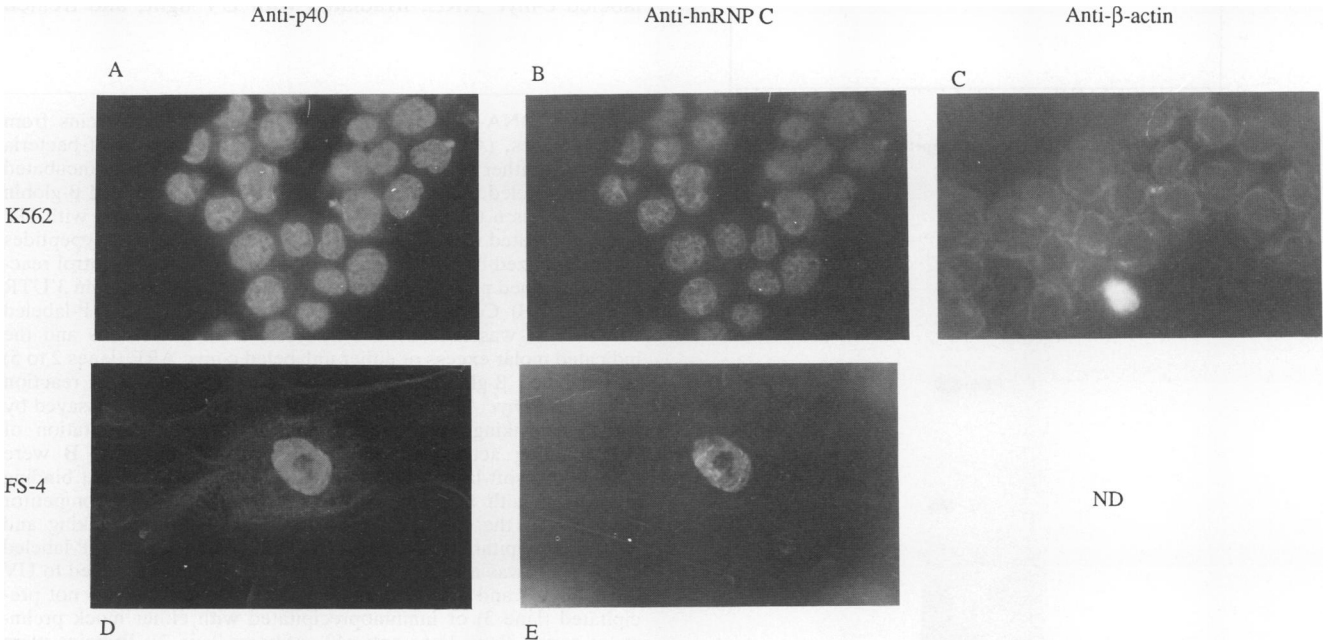

FIG. 6. Localization of AUF1 by indirect immunofluorescence. K562 cells (A to C) or FS-4 human fibroblasts (D and E) were subjected to indirect immunofluorescence as described in Materials and Methods. The antibodies used are indicated at the top. ND, not done.

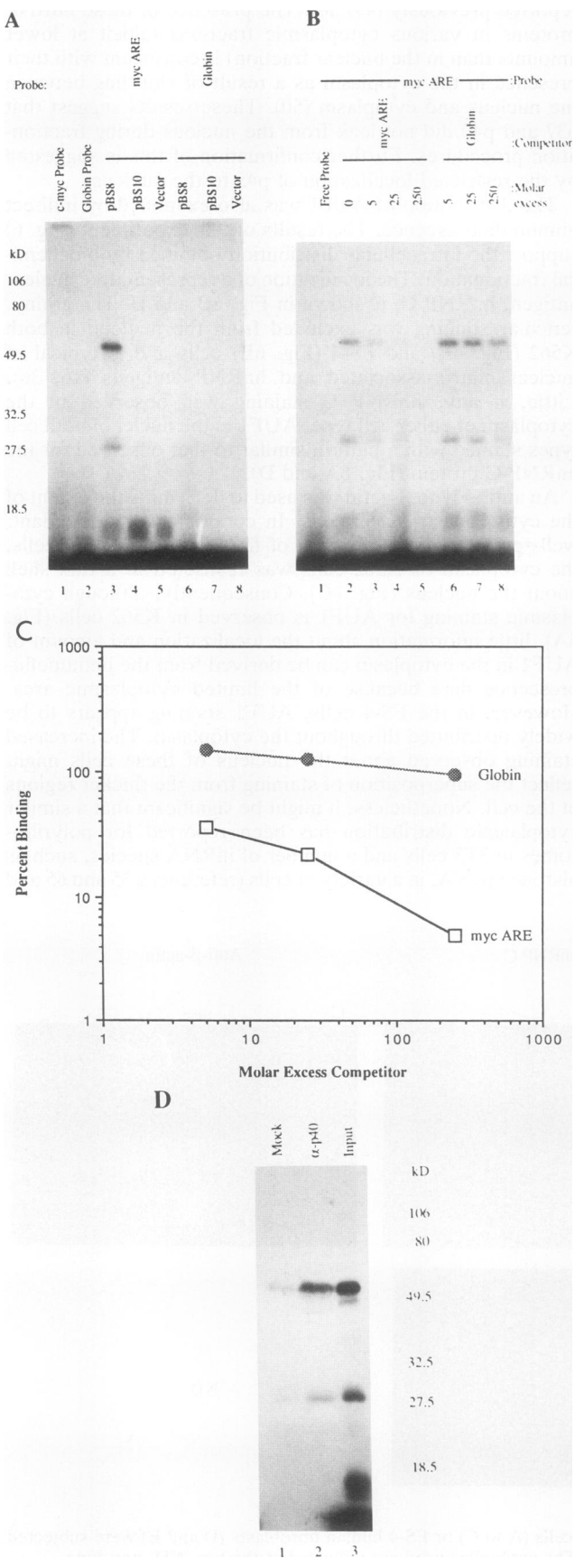

references therein). Together, the biochemical fractionation and immunofluorescence data indicate that AUF1 is located in both the nucleus and the cytoplasm.

Isolation and characterization of an AUF1 cDNA clone. Western blot analysis indicated that AUF1 is present in HeLa cells (data not shown). Screening of 600,000 clones from a HeLa λ ZAP II expression library with affinity-purified α-p40 antibody resulted in the isolation of positive clones, designated pBS8 and pBS10, encoding fusion proteins that reacted with the specific antibody (data not shown). To test ARE-binding activity of the recombinant proteins, bacterial lysates of pBS8, pBS10, or vector alone were used in a UV cross-linking assay with ^{32}P-labeled c-*myc* ARE or ^{32}P-labeled β-globin 3′UTR. The 55-kDa fusion protein (derived by fusion of the β-galactosidase open reading frame with the AUF1 5′UTR and AUF1 open reading frame) encoded by pBS8 specifically cross-linked to the c-*myc* ARE but not β-globin 3′UTR (Fig. 7A; compare lane 3 with lane 6). Moreover, the pBS8 fusion protein bound RNA with the same specificity as did cellular AUF1, using the nine substrates shown in Fig. 1 and 2 (data not shown). In contrast, protein from the pBS10 and vector-only lysates did not support cross-linking to either the c-*myc* ARE or β-globin 3′UTR (Fig. 7A, lanes 4 and 7 or lanes 5 and 8, respectively). Thus, the pBS10 protein contains an epitope allowing cross-reactivity to the α-p40 antibody, but the protein lacks RNA-binding activity. To substantiate the RNA-binding specificity of the BS8 fusion protein, UV cross-linking experiments were performed with protein from BS8, ^{32}P-labeled c-*myc* ARE, and either unlabeled c-*myc* ARE or β-globin 3′UTR as competitors. Unlabeled c-*myc* ARE lowered binding to 5% at 250-fold molar excess, while unlabeled β-globin 3′UTR had little, if any, effect on binding even at 250-fold molar excess (Fig. 7B and C). These data suggested that the BS8 fusion protein binds to AREs but not to β-globin 3′UTR. Direct evidence that pBS8 encodes an ARE-binding protein was obtained by immunoprecipitation of the protein cross-linked to the c-*myc* ARE by using α-p40 antibody. The BS8 bacterial lysate was mixed with ^{32}P-labeled c-*myc* ARE, irradiated with UV light, and treated

FIG. 7. RNA-binding characterization of fusion proteins from cDNA clones. (A) UV cross-linking analysis. Lysates of bacteria containing either pBS8, pBS10, or phagemid vector were incubated with ^{32}P-labeled c-*myc* ARE (lanes 3 to 5) or ^{32}P-labeled β-globin 3′UTR (lanes 6 to 8). Reaction mixtures were irradiated with UV light and treated with RNase A as described for Fig. 1. Polypeptides were visualized by SDS-PAGE and autoradiography. Control reactions contained probes only (c-*myc* ARE [lane 1] or β-globin 3′UTR [lane 2]). (B) Competition analysis of ARE binding. ^{32}P-labeled c-*myc* ARE was incubated with lysate from pBS8 cells and the indicated molar excess of either unlabeled c-*myc* ARE (lanes 2 to 5) or unlabeled β-globin 3′UTR (lanes 6 to 8). A control reaction contained c-*myc* ARE probe only (lane 1). Binding was assayed by UV cross-linking as described for Fig. 1. (C) Quantitation of RNA-binding activity. The 55-kDa bands from panel B were scanned by soft-laser densitometry and plotted as percent binding (compared with no competitor) versus molar excess competitor indicated to the right of each curve. (D) UV cross-linking and immunoprecipitation analysis of fusion protein pBS8. ^{32}P-labeled c-*myc* ARE was mixed with lysate from pBS8 and subjected to UV cross-linking and RNase treatment. Mixtures were either not precipitated (lane 3) or immunoprecipitated with either mock preimmune serum (lane 1) or anti-p40 antibody (lane 2). Proteins were visualized by SDS-PAGE and autoradiography. Molecular sizes of markers are indicated for each autoradiograph.

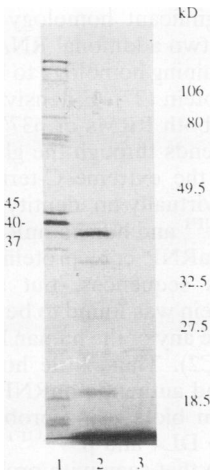

FIG. 8. In vitro translation of RNA from AUF1 clone pBS8. RNA synthesized from clone pBS8 was used to program protein synthesis in a reticulocyte lysate in the presence of [^{35}S]methionine. For comparison, immunoprecipitation of proteins from a lysate of K562 cells metabolically labeled with [^{35}S]methionine with α-p40 antibody was also performed. Products were separated by SDS-PAGE (10% gel) and visualized by autoradiography. The molecular sizes of marker proteins are shown at the right; the locations of the p37, p40, and p45 in immunoprecipitates are shown at the left. Lanes: 1, immunoprecipitation of proteins from a lysate of K562 cells metabolically labeled with [^{35}S]methionine, using α-p40; 2, in vitro translation with AUF1 RNA synthesized in vitro by using T7 RNA polymerase; 3, in vitro translation in the absence of added RNA.

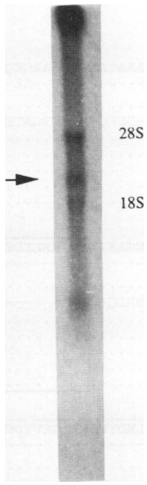

FIG. 9. Northern blot analysis of AUF1 mRNA. Five micrograms of poly(A)$^+$ RNA from K562 cells was analyzed by Northern blot assay as described previously (11), using a ^{32}P-labeled p37^{AUF1} probe from the 3′UTR. The positions of 28S and 18S rRNAs are indicated. The 2.5-kb AUF1 mRNA is indicated by the arrow.

with RNase A. The mixture was immunoprecipitated with α-p40 or mock-purified preimmune antibody. Protein was visualized by SDS-PAGE and autoradiography. Reactions with α-p40 precipitated the 55-kDa fusion protein fourfold more efficiently than the control reactions did (Fig. 7D), indicating that the BS8 fusion protein is an ARE-binding protein recognized by the α-p40/AUF1 antibody.

To determine which polypeptide species of AUF1 is encoded by the pBS8 cDNA, an in vitro translation experiment was performed. pBS8 cDNA was used as a template for RNA synthesis by T7 RNA polymerase. This RNA was used to program protein synthesis in a reticulocyte lysate in the presence of [^{35}S]methionine. Translation produced a major 37-kDa species (Fig. 8, lane 2) which comigrates with p37^{AUF1} in immunoprecipitates of lysates from K562 cells metabolically labeled with [^{35}S]methionine (lane 1). As a control, translation without added RNA resulted in no detectable polypeptide products in this size range (lane 3). Taken together, these data strongly suggest that the pBS8 cDNA corresponds to the 37-kDa species of AUF1. Therefore, this cDNA is hereafter referred to as p37^{AUF1}.

Sequence analysis of p37^{AUF1}. p37^{AUF1} (pBS8) was sequenced completely on both strands. The cDNA is 2,562 bp in length. A single open reading frame was consistent with the production of a β-galactosidase fusion protein in the phage isolate. The first ATG at position 246 is in a good context for initiation of translation, with an A at position −3 (29). Assuming that this is the authentic initiation codon, the open reading frame extends to position 1106 and encodes a polypeptide with a predicted M_r of 32,000. The 5′UTR is at least 245 nt in length. The cDNA should not be significantly larger than 2.5 kb, since Northern (RNA) blot analysis of poly(A)$^+$ RNA from K562 cells reveals a band of approximately 2.5 kb in addition to some cross-hybridization with contaminating 28S and 18S rRNAs (Fig. 9). The 3′UTR is unusually long (at least 1.4 kb) and contains one ATTAAA polyadenylation signal (51) at position 1799. There is most likely an additional polyadenylation signal not present in the cDNA, since Northern analysis indicates that p37^{AUF1} mRNA is approximately 2.5 kb in length. Typically, a proximal polyadenylation site is used at 5 to 20% of the efficiency of a distal site (reference 34 and references therein). The 3′UTR of p37^{AUF1} cDNA contains three ATTTA and two ATTTTA motifs.

The MOTIFS subroutine of the Genetics Computer Group software was used to analyze the p37^{AUF1} cDNA sequence. p37^{AUF1} contains phosphorylation sites for cyclic AMP-dependent protein kinase, protein kinase C, casein kinase II, and tyrosine phosphokinase (26). p37^{AUF1} contains two RNP consensus-type RNA-binding motifs also referred to as RNA recognition motifs (RRMs) (Fig. 10) (4, 23, 42, 75). An RRM is a 90-amino-acid domain containing a conserved 8-amino-acid consensus sequence, (R/K)GF(G/A)FVX(F/Y), referred to as RNP-1, and a less conserved 6-amino-acid motif, referred to as RNP-2. Structural studies indicate that an RRM consists of a four-stranded antiparallel β sheet with two α helices packed against one face of the sheet (reviewed in reference 75). RNP-1 and RNP-2 lie on the central two strands at the center of the β sheet. RRMs are found in three types of RNA-binding proteins: hnRNPs, splicing regulators, and development stage-specific factors (28). The C-terminal end of p37^{AUF1} contains a glutamine-rich motif (KEQYQQQQQWGSRGG; Fig. 10). These motifs are thought to serve as protein-protein interaction sites in some RNA- and DNA-binding proteins (4, 18).

Homology of p37^{AUF1} to other RNA-binding proteins. Data base sequence comparisons with p37^{AUF1} revealed regions of significant nucleotide and amino acid homology with several RNA-binding proteins. The optimal alignments are shown in Fig. 10. Most notable is DL4, a partial cDNA which appears to encode a protein that cross-reacts with antibodies to hnRNP C (32). The DL4 sequence shown contains several corrections from the published GenBank

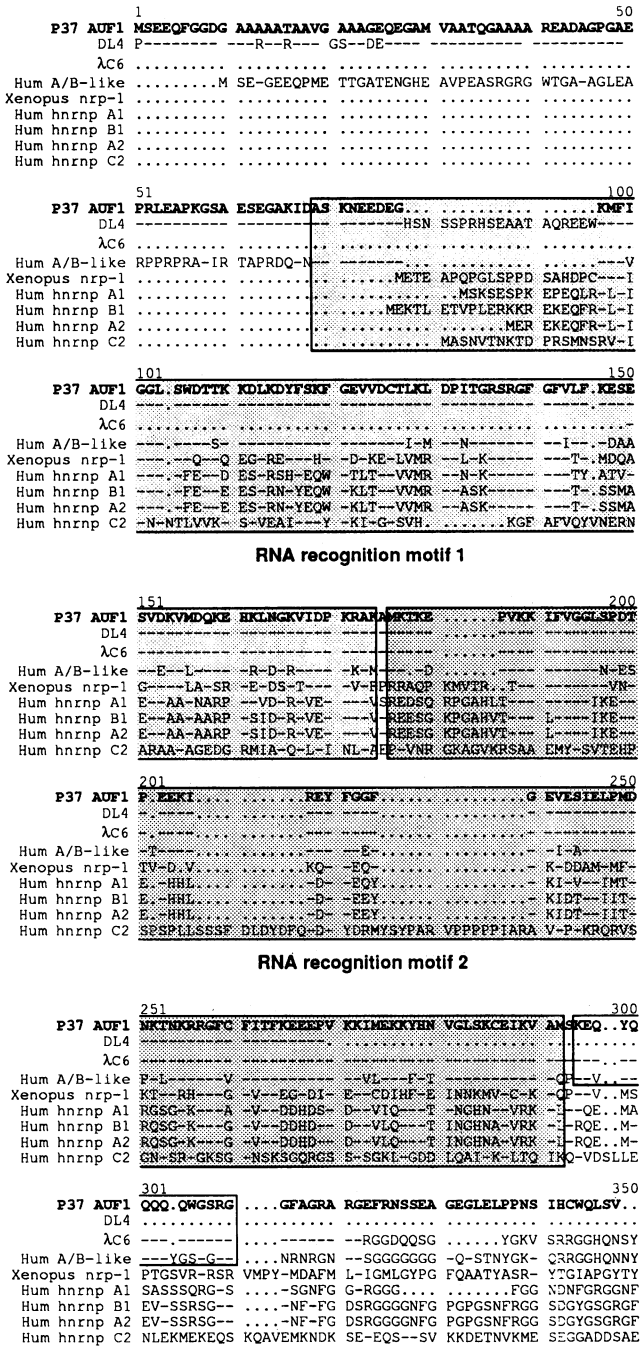

FIG. 10. Amino acid homologies between p37^{AUF1} and selected RNA-binding proteins. Alignment of amino acid sequences was computed by the PILEUP subroutine of the Genetics Computer Group software. The sequence of p37^{AUF1} is listed. For the proteins used for comparison, identical amino acids are indicated by dashes and gaps are indicated by dots. Three regions of p37^{AUF1} are highlighted: two putative RRMs (shaded boxes) (4) and a glutamine-rich domain immediately C terminal to the second RRM (boxed). The GenBank accession numbers for the proteins are as follows: DL4, X03910; λC6, X16933; human (Hum) hnRNP A/B-related protein, M65028; *Xenopus* rnp-1, M34894; human hnRNP A1, X12671; human hnRNP B1, M29064; human hnRNP A2, M29065; human hnRNP C2, M29063.

sequence (37a). Significant homology is also evident between p37^{AUF1} and two additional RNA-binding proteins: a rat clone, λC6, containing homology to DL4 (63), and human hnRNP A/B-like protein (27). Extensive homology (77%) is evident throughout both RRMs of p37^{AUF1}, λC6, and A/B-like protein and extends through the glutamine-rich domain (>87%). However, the extreme C-terminal sequences are unrelated. There is virtually no identity seen in the N-terminal domain of p37^{AUF1} and human hnRNP A/B-like protein. Several authentic hnRNP core proteins scored among the top 40 homologous sequences, but a *Xenopus* nervous system-specific protein was found to be more closely related to p37^{AUF1} than were any of the human hnRNP core proteins (A1, B1, A2, and C2). Thus, little homology is observed between p37^{AUF1} and authentic hnRNP core proteins.

Genomic Southern blots using probes derived from sequences common to DL4 and p37^{AUF1} reveal a more complicated pattern than that seen with probes derived from the 3′UTR region of p37^{AUF1} (70a). Thus, we are currently investigating the hypothesis that the RRM of p37^{AUF1} defines a family of related proteins that may include the p40 and p45 polypeptides described in this report, the DL4 protein, the human homolog of λC6, and the human hnRNP A/B-like protein (70a). This finding would be consistent with recent studies of RRM-containing proteins in *Drosophila melanogaster* in which isolation of 12 different RRM clones revealed three families of RRM-containing proteins consisting of developmental stage-specific proteins, splicing factors, and hnRNP proteins (28). In conclusion, the combined immunological characterization and sequence data demonstrate that p37^{AUF1} is an ARE-binding protein distinct from the hnRNP A, B, or C protein.

DISCUSSION

We are purifying candidate proteins that regulate or contribute to the degradation of specific mRNAs. Our long-term goal is to reconstitute ARE-directed mRNA degradation from components purified to homogeneity. This will permit stringent control of reaction conditions, concentrations of enzymes and substrates, and their order of addition. Only this, in turn, will permit the contributions of individual components and their interactions to be studied (71). To this end, we have purified, characterized, and molecularly cloned an ARE RNA-binding protein, AUF1, whose binding specificity suggests its involvement in ARE-directed mRNA degradation in cells. Specifically, we have tested the minimal sequences that govern rapid decay for three different mRNAs: those for c-*fos*, c-*myc*, and GM-CSF (reviewed in reference 60). The best characterized is c-*fos*, in which case insertion of the 75-nt ARE into rabbit β-globin mRNA causes rapid decay in vivo and confers AUF1 binding in vitro. In the case of c-*myc*, deletion of the AUF1-binding region from the 3′UTR stabilizes the mRNA (25). In the case of GM-CSF, insertion of the AUF1-binding region into rabbit β-globin mRNA causes its rapid decay in vivo (60). In contrast, the rabbit β-globin 3′UTR does not destabilize an mRNA, and AUF1 does not bind this sequence. Taken together, these data strongly suggest that AUF1 functions in turnover of these mRNAs. Moreover, rapid deadenylation of chimeric β-globin/c-*fos* ARE mRNA does not require intact AUUUA motifs (64); likewise, binding of AUF1 does not require intact AUUUA motifs in the c-*myc* and c-*fos* AREs (Fig. 1). However, more work will be required to determine whether AUF1 participates in the deadenylation step of ARE-directed mRNA degradation.

One possible mechanism by which AUF1 participates in mRNA degradation is through interaction of AUF1 with both the ARE and other proteins (e.g., pp55, p75, pp106, p120, or p126; Fig. 4) that might associate with the poly(A) tract or poly(A)-binding protein (PAB). This might have the effect of increasing the affinity of a poly(A) nuclease for poly(A) tracts linked to mRNAs containing an ARE (38). Alternatively, the binding of AUF1 to the ARE and its interaction with other proteins might alter the affinity of PAB for the poly(A) tract, thus increasing its susceptibility to RNase(s) (6). Concerning the ability of AUF1 to associate with other proteins, it is noteworthy that the $p37^{AUF1}$ cDNA sequence predicts a polypeptide with a glutamine-rich motif, KEQYQQQQQWGSRGG (boxed in Fig. 10). Glutamine-rich regions are thought to mediate protein-protein interactions and are present in some RNA- and DNA-binding proteins (4).

Resolution of the mechanism(s) by which AUF1 mediates the ARE-directed degradation pathway will, of course, require the reconstitution of c-*myc* mRNA degradation in vitro using purified components. Several observations suggest that the identification and purification of factors in addition to AUF1 will be required to realize this reconstitution in vitro. (i) AUF1 purified by RNA affinity chromatography (this report) is insufficient to enhance degradation of polysome-bound c-*myc* mRNA in vitro (data not shown). This is not surprising given the high salt concentrations (3.5 M) required to elute AUF1 from the poly(U)-agarose column. Future work will be required to determine the extent to which multiple chromatographic fractions restore mRNA degradation activity in vitro. Historically, a similar situation occurred during fractionation of nuclear extracts competent for RNA cleavage/polyadenylation activity in vitro; reconstitution of activity required recombination of multiple chromatographic fractions as single fractions had no activity (43). (ii) c-*myc* mRNA, and its poly(A) tract, are stable in cell-free mRNA decay reactions supplemented with S130, using polysomes salt washed under conditions that both solubilize polysome-associated AUF1 (data not shown) and maintain the integrity of the ribosome (54). (AUF1 fractionates with polysomes and S130 [Fig. 5].) Moreover, removal of greater than 95% of AUF1 from S130 by immunoprecipitation does not affect the destabilizing activity of S130 for c-*myc* mRNA in cell-free decay reactions (data not shown), suggesting that AUF1 might be a necessary, but not sufficient, cofactor in the degradation machinery. However, interpretation of this AUF1 depletion result is complicated by the fact that endogenous, polysome-associated c-*myc* mRNA contains a coding region instability determinant (reviewed in reference 60) which might be responsive to factors still present in AUF1-depleted S130. Clearly, further fractionation of polysomes and S130 will be required to purify additional factors. (iii) In this regard, p75, p120, p126, pp55, and pp106 coimmunoprecipitate reproducibly with AUF1 (Fig. 4), suggesting that AUF1 can associate with other cellular proteins. More work will be required to ascertain any significance of these additional proteins. However, it is noteworthy that degradation of AU-rich mRNAs might be mediated by assembly of a >20S degradation complex (59). AUF1 is one likely candidate as a component of this complex. Additional candidate proteins for this putative complex are PAB (6, 56), poly(A) nuclease(s) (2, 38, 57), and RNases that could degrade specific mRNA sequences (53). The relevance of PAB is highlighted by studies suggesting that in vitro deadenylation of yeast *MFA2* mRNA requires purified yeast poly(A) nuclease, PAB, and a specific AU-rich sequence located in the *MFA2* 3'UTR (38). Indeed, the striking similarities of deadenylation mediated by the *MFA2* AU-rich sequence and mRNAs with AREs in higher eukaryotes have been noted, suggesting that the yeast AU-rich sequence might be analogous to the ARE (38, 44).

Given the putative role(s) of AUF1 in cytoplasmic mRNA degradation, what is a rationale for its nuclear and cytoplasmic localization (Fig. 5 and 6)? It could be involved in both nuclear and cytoplasmic RNA turnover. Alternatively, AUF1 could bind to the ARE in the nucleus to facilitate transport of the mRNP to the cytoplasm, where its degradation would also be controlled by AUF1. In this regard it is noteworthy that an ARE can facilitate nucleocytoplasmic transport of the mRNA in an ATP-dependent manner in cell extracts (45). Mechanistically, this is thought to occur by an ARE-binding protein that increases the affinity of the ARE-linked mRNA for a nuclear, 106-kDa, phosphorylated PAB representing a putative carrier for mRNA transport (61). More work will be required to determine whether this phosphorylated PAB is related to the 106-kDa phosphoprotein which coimmunoprecipitates with AUF1 (Fig. 4).

Consistent with the nuclear and cytoplasmic localization of AUF1 is the observation that other RNA-binding proteins are nuclear and cytoplasmic as well (reference 66 and references therein). We cite several examples. PABs are nuclear and cytoplasmic (55). hnRNP A1 is predominantly nuclear; however, low levels are cytoplasmic as a result of shuttling between both compartments. When in the cytoplasm, A1 is bound to mRNA, and RNA polymerase II transcription is required before it can return to the nucleus (49, 50). The glycolytic enzyme glyceraldehyde-3-phosphate dehydrogenase binds tRNAs in a sequence-specific manner in the nucleus and performs its glycolytic functions in the cytoplasm (66). Finally, a 50-kDa protein which binds to the histone mRNA stem-loop structure in the nucleus is complexed with the mRNA in polyribosomes (47). The histone stem-loop is also required for both transport of the mRNA to the cytoplasm and its localization to polyribosomes (67). Perhaps these processes are facilitated by the 50-kDa protein. In summary, these studies indicate that cytoplasmic and nuclear localization of AUF1 is not inconsistent with characteristics of other RNA-binding proteins.

In conclusion, we have characterized and cloned an ARE-binding protein which may mediate ARE-directed mRNA degradation. Further studies will be required to determine the extent to which it interacts with other components of the mRNA degradation machinery to effect this RNA processing pathway. The antibodies to AUF1 and the cDNA described in this report will be valuable reagents for further dissection of the ARE-directed mRNA degradation pathway.

ACKNOWLEDGMENTS

The first three authors contributed equally to this work.

We thank Nina Allen for the use of fluorescent microscopes; Ann-Bin Shyu, Gray Shaw, and John Thomas for plasmids; Jeff Wilusz for monoclonal antibodies; Barbara Yoza for the HeLa cDNA library; and Allan Jacobson, Doug Lyles, David Ornelles, Roy Parker, Stu Peltz, Roger Perlmutter, Jeff Ross, and Alan Sachs for helpful discussions.

This work was supported by Public Health Service grant CA52443 from the National Cancer Institute and by a grant from the Life and Health Insurance Medical Research Fund to G.B. K.E. is supported by postdoctoral training grant T32-AI07401 from the NIH. B.J.W. is supported by NRSA grant DK08589 from the NIH.

REFERENCES

1. **Akashi, M., G. Shaw, M. Gross, M. Saito, and H. P. Koeffler.** 1991. Role of AUUU sequences in stabilization of granulocyte-macrophage colony-stimulating factor RNA in stimulated cells. Blood **78**:2005–2012.
2. **Åström, J., A. Åström, and A. Virtanen.** 1991. In vitro deadenylation of mammalian mRNA by a HeLa cell 3′ exonuclease. EMBO J. **10**:3067–3071.
3. **Atwater, J. A., R. Wisdom, and I. M. Verma.** 1990. Regulated mRNA stability. Annu. Rev. Genet. **24**:519–541.
4. **Bandzuilis, R. J., M. S. Swanson, and G. Dreyfuss.** 1989. RNA-binding proteins as developmental regulators. Genes Dev. **3**:431–437.
5. **Battey, J., C. Moulding, R. Taub, W. Murphy, T. Stewart, H. Potter, G. Lenoir, and P. Leder.** 1983. The human c-myc oncogene: structural consequences of translocation into the IgH locus in Burkitt lymphoma. Cell **34**:779–787.
6. **Bernstein, P., S. W. Peltz, and J. Ross.** 1989. The poly(A)-poly(A)-binding protein complex is a major determinant of mRNA stability in vitro. Mol. Cell. Biol. **9**:659–670.
7. **Bickel, M., Y. Iwai, D. H. Pluznik, and R. B. Cohen.** 1992. Binding of sequence-specific proteins to the adenosine- plus uridine-rich sequences of the murine granulocyte/macrophage colony-stimulating factor mRNA. Proc. Natl. Acad. Sci. USA **89**:10001–10005.
8. **Bohjanen, P. R., B. Petryniak, C. H. June, C. B. Thompson, and T. Lindsten.** 1991. An inducible cytoplasmic factor (AU-B) binds selectively to AUUUA multimers in the 3′ untranslated region of lymphokine mRNA. Mol. Cell. Biol. **11**:3288–3295.
9. **Bohjanen, P. R., B. Petryniak, C. H. June, C. B. Thompson, and T. Lindsten.** 1992. AU RNA-binding factors differ in their binding specificities and affinities. J. Biol. Chem. **267**:6302–6309.
10. **Brewer, G.** 1991. An A+U-rich element RNA binding factor regulates c-myc mRNA stability in vitro. Mol. Cell. Biol. **11**:2460–2466.
11. **Brewer, G., and J. Ross.** 1988. Poly(A) shortening and degradation of the 3′ AU-rich sequences of human c-myc mRNA in a cell-free system. Mol. Cell. Biol. **8**:1697–1708.
12. **Brewer, G., and J. Ross.** 1989. Regulation of c-myc mRNA degradation in vitro by a labile destabilizer with an essential nucleic acid component. Mol. Cell. Biol. **9**:1996–2006.
13. **Brewer, G., and J. Ross.** 1990. Messenger RNA turnover in cell-free extracts. Methods Enzymol. **181**:202–209.
14. **Burd, C. G., M. S. Swanson, M. Görlach, and G. Dreyfuss.** 1989. Primary structures of the heterogenous nuclear ribonucleoprotein A2, B1, and C2 proteins: a diversity of RNA binding proteins is generated by small peptide inserts. Proc. Natl. Acad. Sci. USA **86**:9788–9792.
15. **Buvoli, M., G. Biamonti, P. Tsoulfas, M. T. Bassi, A. Ghetti, S. Riva, and C. Morandi.** 1988. cDNA cloning of human hnRNP protein A1 reveals the existence of multiple mRNA isoforms. Nucleic Acids Res. **16**:3751–3770.
16. **Chaly, N., M. P. Sabour, J. C. Silver, W. A. Aitchison, J. E. Little, and D. L. Brown.** 1986. Monoclonal antibodies against nuclear antigens in mammalian, insect and plant cells: an immunofluorescence study. Cell Biol. Int. Rep. **10**:421–428.
17. **Cole, M. D.** 1986. The myc oncogene: its role in transformation and differentiation. Annu. Rev. Genet. **20**:361–384.
18. **Courey, A. J., and R. Tjian.** 1988. Analysis of Sp1 in vivo reveals multiple transcriptional domains, including a novel glutamine-rich activation motif. Cell **55**:887–898.
19. **Dani, C., J. M. Blanchard, M. Piechaczyk, S. El Sabouty, L. Marty, and P. Jeanteur.** 1984. Extreme instability of myc mRNA in normal and transformed human cells. Proc. Natl. Acad. Sci. USA **81**:7046–7050.
20. **Davidson, E. H.** 1986. Gene activity in early development, 3rd ed. Academic Press, Orlando, Fla.
21. **Dean, A., T. J. Ley, R. K. Humphries, M. Fordis, and A. N. Schecter.** 1983. Inducible transcription of five globin genes in K562 human leukemia cells. Proc. Natl. Acad. Sci. USA **80**:5515–5519.
22. **Evans, E. A.** 1986. The purification and characterization of microsomal signal peptidase, p. 87–89. Ph.D. thesis. The Rockefeller University, New York, N.Y.
23. **Frankel, A. D., I. W. Mattaj, and D. C. Rio.** 1991. RNA-protein interactions. Cell **67**:1041–1046.
24. **Hamilton, B. J., E. Nagy, J. S. Malter, B. A. Arrick, and W. F. C. Rigby.** 1993. Association of heterogenous nuclear ribonucleoprotein A1 and C proteins with reiterated AUUUA sequences. J. Biol. Chem. **268**:8881–8887.
25. **Jones, T. R., and M. D. Cole.** 1987. Rapid cytoplasmic turnover of c-myc mRNA: requirement of the 3′ untranslated sequences. Mol. Cell. Biol. **7**:4513–4521.
26. **Kemp, B. E., and R. B. Pearson.** 1990. Protein kinase recognition sequence motifs. Trends Biochem. Sci. **15**:342–346.
27. **Khan, F., A. K. Jaiswal, and W. Szer.** 1991. Cloning and sequence analysis of a human type A/B hnRNP protein. FEBS Lett. **290**:159–161.
28. **Kim, Y.-J., and B. S. Baker.** 1993. Isolation of RRM-type RNA-binding protein genes and the analysis of their relatedness by using a numerical approach. Mol. Cell. Biol. **13**:174–183.
29. **Kozak, M.** 1991. Structural features in eukaryotic mRNAs that modulate the initiation of translation. J. Biol. Chem. **266**:19867–19870.
30. **Kruys, V., O. Marinx, G. Shaw, J. Deschamps, and G. Huez.** 1989. Translational blockade imposed by cytokine-derived UA-rich sequences. Science **245**:852–855.
31. **Kumar, A., K. R. Williams, and W. Szer.** 1986. Purification and domain structure of core hnRNP proteins A1 and A2 and their relationship to single-stranded DNA-binding proteins. J. Biol. Chem. **261**:11266–11273.
32. **Lahiri, D. K., and J. O. Thomas.** 1986. A cDNA clone of the hnRNP C proteins and its homology with the single-stranded DNA binding protein UP2. Nucleic Acids Res. **14**:4077–4094.
33. **Laird-Offringa, I. A.** 1992. What determines the instability of c-myc proto-oncogene mRNA? BioEssays **14**:119–124.
34. **Laird-Offringa, I. A., P. Elfferich, H. J. Knaken, J. de Ruiter, and A. J. van der Eb.** 1989. Analysis of polyadenylation site usage of the c-myc oncogene. Nucleic Acids Res. **17**:6499–6514.
35. **Lawrence, J. B., R. H. Singer, and L. M. Marselle.** 1989. Highly localized tracks of specific transcripts within interphase nuclei visualized by in situ hybridization. Cell **57**:493–502.
36. **Lehner, C. F., H. M. Eppenberger, S. Fakan, and E. A. Nigg.** 1986. Nuclear substructure antigens. Monoclonal antibodies against components of nuclear matrix preparations. Exp. Cell Res. **162**:205–219.
37. **Lindsten, T., C. H. June, J. A. Ledbetter, G. Stella, and C. B. Thompson.** 1989. Regulation of lymphokine messenger RNA stability by a surface-mediated T cell activation pathway. Science **244**:339–342.

37a. **Long, L., B. J. Wagner, and G. Brewer.** Unpublished data.

38. **Lowell, J. E., D. Z. Rudner, and A. B. Sachs.** 1992. 3′-UTR-dependent deadenylation by the yeast poly(A) nuclease. Genes Dev. **6**:2088–2099.
39. **Lozzio, C. B., and B. B. Lozzio.** 1975. Human chronic myelogenous leukemic cell line with positive Philadelphia chromosome. Blood **45**:321–334.
40. **Malter, J. S.** 1989. Identification of an AUUUA-specific messenger RNA binding protein. Science **246**:664–666.
41. **Marcu, K. B., S. A. Bossone, and A. J. Patel.** 1992. myc function and regulation. Annu. Rev. Biochem. **61**:809–860.
42. **Mattaj, I. W.** 1989. A binding consensus: RNA-protein interactions in splicing, snRNPs and sex. Cell **57**:1–3.
43. **McDevitt, M. A., G. M. Gilmartin, W. H. Reeves, and J. R. Nevins.** 1988. Multiple factors are required for poly(A) addition to a mRNA 3′ end. Genes Dev. **2**:588–597.
44. **Muhlrad, D., and R. Parker.** 1992. Mutations affecting stability and deadenylation of the yeast MFA2 transcript. Genes Dev. **6**:2100–2111.
45. **Müller, W. E. G., H. Slor, K. Pfeifer, P. Hühn, A. Bek, S. Orsulic, H. Ushijima, and H. C. Schröder.** 1992. Association of AUUUA-binding protein with A+U-rich mRNA during nucleocytoplasmic transport. J. Mol. Biol. **226**:721–733.
46. **Myer, V. E., S. I. Lee, and J. A. Steitz.** 1992. Viral small nuclear ribonucleoproteins bind a protein implicated in messenger RNA

destabilization. Proc. Natl. Acad. Sci. USA **89:**1296–1300.
47. **Pandey, N. B., J.-H. Sun, and W. F. Marzluff.** 1991. Different complexes are formed on the 3′ end of histone mRNA with nuclear and polysomal proteins. Nucleic Acids Res. **19:**5653–5659.
48. **Peltz, S. W., G. Brewer, P. Bernstein, P. A. Hart, and J. Ross.** 1991. Regulation of mRNA turnover in eukaryotic cells. Crit. Rev. Euk. Gene Expression **1:**99–126.
49. **Pinol-Roma, S., and G. Dreyfuss.** 1991. Transcription-dependent and transcription-independent nuclear transport of hnRNP proteins. Science **253:**312–314.
50. **Pinol-Roma, S., and G. Dreyfuss.** 1992. Shuttling of pre-mRNA binding proteins between nucleus and cytoplasm. Nature (London) **355:**730–732.
51. **Proudfoot, N.** 1991. Poly(A) signals. Cell **64:**671–674.
52. **Richter, K., P. J. Good, and I. B. Dawid.** 1990. A developmentally regulated, nervous system-specific gene in Xenopus encodes a putative RNA-binding protein. New Biol. **2:**556–565.
53. **Ross, J.** 1993. mRNA decay in cell-free systems, p. 417–448. *In* G. Brawerman and J. Belasco (ed.), Control of messenger RNA stability. Academic Press, New York.
54. **Ross, J., G. Kobs, G. Brewer, and S. W. Peltz.** 1987. Properties of the exonuclease activity that degrades H4 histone mRNA. J. Biol. Chem. **262:**9374–9381.
55. **Sachs, A. B., M. W. Bond, and R. D. Kornberg.** 1986. A single gene from yeast for both nuclear and cytoplasmic polyadenylate-binding proteins: domain structure and expression. Cell **45:**827–835.
56. **Sachs, A. B., and R. W. Davis.** 1989. The poly(A) binding protein is required for poly(A) shortening and 60S ribosomal subunit-dependent translation initiation. Cell **58:**857–867.
57. **Sachs, A. B., and J. A. Deardorff.** 1992. Translation initiation requires the PAB-dependent poly(A) ribonuclease in yeast. Cell **70:**961–973.
58. **Sambrook, J., E. F. Fritsch, and T. Maniatis.** 1989. Molecular cloning: a laboratory manual, 2nd ed. Cold Spring Harbor Laboratory Press, Cold Spring Harbor, N.Y.
59. **Savant-Bhonsale, S., and D. W. Cleveland.** 1992. Evidence for instability of mRNAs containing AUUUA motifs mediated through translation-dependent assembly of a >20S degradation complex. Genes Dev. **6:**1927–1939.
60. **Schiavi, S. C., J. G. Belasco, and M. E. Greenberg.** 1992. Regulation of proto-oncogene mRNA stability. Biochim. Biophy. Acta **1114:**95–106.
61. **Schröder, H. C., M. Rottmann, R. Wenger, M. Bachmann, A. Dorn, and W. E. G. Müller.** 1988. Studies on protein kinases involved in regulation of nucleocytoplasmic mRNA transport. Biochem. J. **252:**777–790.
62. **Schuler, G. D., and M. D. Cole.** 1988. GM-CSF and oncogene mRNA stabilities are independently regulated in trans in a mouse monocytic tumor. Cell **55:**1115–1122.
63. **Sharp, Z. D., K. P. Smith, Z. Cao, and S. Helsel.** 1990. Cloning of the nucleic acid-binding domain of the rat hnRNP C-type protein. Biochim. Biophys. Acta **1048:**306–309.
64. **Shyu, A.-B., J. G. Belasco, and M. E. Greenberg.** 1991. Two distinct destabilizing elements in the c-fos message trigger deadenylation as a first step in rapid mRNA decay. Genes Dev. **5:**221–231.
65. **Singer, R. H., G. L. Langevin, and J. B. Lawrence.** 1989. Ultrastructural visualization of cytoskeletal mRNAs and their associated proteins using double-label in situ hybridization. J. Cell Biol. **108:**2343–2353.
66. **Singh, R., and M. R. Green.** 1993. Sequence-specific binding of transfer RNA by glyceraldehyde-3-phosphate dehydrogenase. Science **259:**365–368.
67. **Sun, J., D. R. Pilch, and W. F. Marzluff.** 1992. The histone mRNA 3′ end is required for localization of histone mRNA to polyribosomes. Nucleic Acids Res. **20:**6057–6066.
68. **Swartwout, S. G., and A. J. Kinniburgh.** 1989. c-*myc* mRNA degradation in growing and differentiating cells: possible alternate pathways. Mol. Cell. Biol. **9:**288–295.
69. **Vakalopoulou, E., J. Schaack, and T. Shenk.** 1991. A 32-kilodalton protein binds to AU-rich domains in the 3′-untranslated regions of rapidly degraded mRNAs. Mol. Cell. Biol. **11:**3355–3364.
70. **Vriz, S., and M. Méchali.** 1989. Analysis of 3′-untranslated regions of seven c-myc genes reveals conserved elements prevalent in post-transcriptionally regulated genes. FEBS Lett. **251:**201–206.
70a. **Wagner, B. J., et al.** Unpublished data.
71. **Wahle, E.** 1992. The end of the message: 3′-end processing leading to polyadenylated messenger RNA. BioEssays **14:**113–118.
72. **Wilson, T., and R. Treisman.** 1988. Removal of poly(A) and consequent degradation of c-fos mRNA facilitated by 3′ AU-rich sequences. Nature (London) **336:**396–399.
73. **Wilusz, J., and T. Shenk.** 1990. A uridylate tract mediates efficient heterogeneous nuclear ribonucleoprotein C protein-RNA cross-linking and functionally substitutes for the downstream element of the polyadenylation signal. Mol. Cell. Biol. **10:**6397–6407.
74. **You, Y., C.-Y. A. Chen, and A.-B. Shyu.** 1992. U-rich sequence-binding proteins interacting with a 20-nucleotide U-rich sequence in the 3′ untranslated region of c-*fos* mRNA may be involved in the first step of c-*fos* mRNA degradation. Mol. Cell. Biol. **12:**2931–2940.
75. **Zamore, P. D., M. L. Zapp, and M. R. Green.** 1990. RNA binding: βs and basics. Nature (London) **348:**485–486.
76. **Zapp, M. L., and M. R. Green.** 1989. Sequence-specific RNA binding by the HIV-1 Rev protein. Nature (London) **342:**714–716.